Electronic supplementary information

MOF-derived lithiophilic CuO nanorod arrays for stable lithium metal anode

Lei Wei,[a] Li Li,[a,b] Teng Zhao,[a] Nanxiang Zhang,[a] Yuanyuan Zhao,[a] Feng Wu[a,b] and Renjie Chen*[a,b]*

a. School of Materials Science & Engineering, Beijing Institute of Technology, Beijing 100081, China.

b. Collaborative Innovation Center of Electric Vehicles in Beijing, Beijing 100081, China.

E-mail address: chenrj@bit.edu.cn (R. Chen); tz270@bit.edu.cn.

Supplementary figures

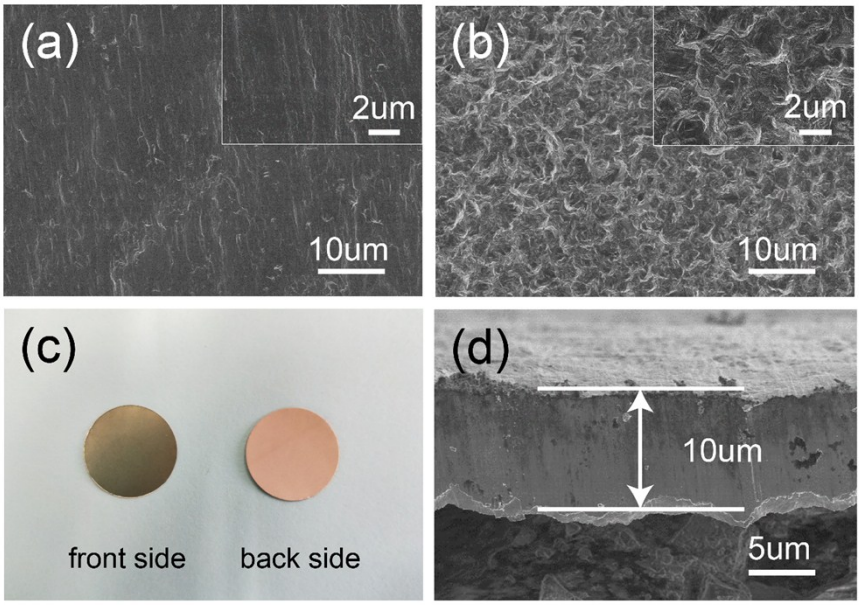

Fig. S1 Top view SEM images of planar Cu foil (a) front side (b) back side. (c) Digital photograph of planar Cu foil. (d) Cross-section SEM image of bare Cu foil. The thickness of Cu foil is about 10um.The inset of (a) and (b) show the high magnification images.

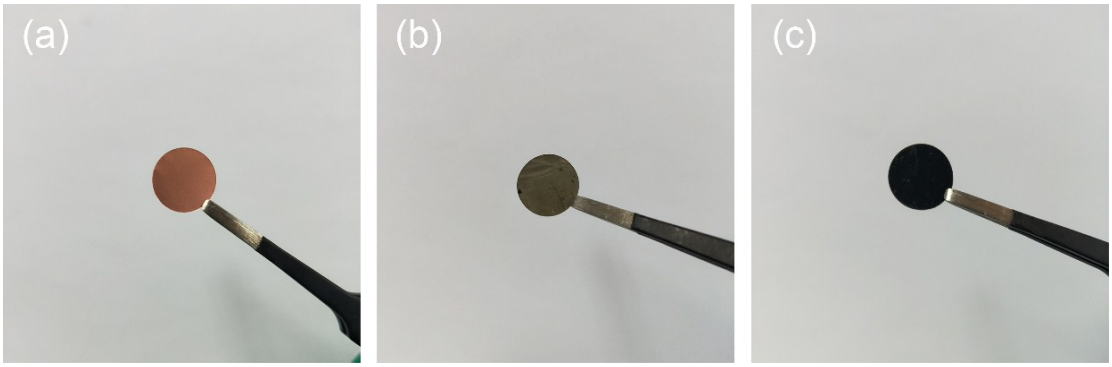

Fig. S2 Opitical images of the color changes for bare Cu foil during the synthesis process.(a) Planar Cu. (b) Cu-TCNQ/CF. (c) CuO NAs/CF

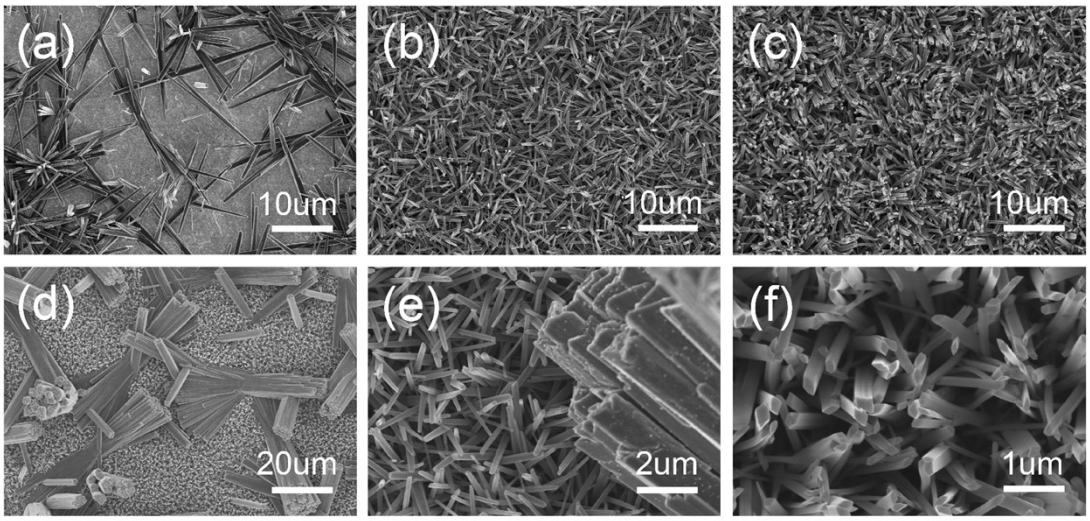

Fig. S3 SEM images of Cu-TCNQ/CF in a concentration of 0.5mM TCNQ acetonitrile solution with different reaction times. (a) 6h (b) 12h (c) 24h. SEM images of Cu-TCNQ/CF in a concentration of 1mM TCNQ acetonitrile solution with (d-e) 6h (f) 12h.

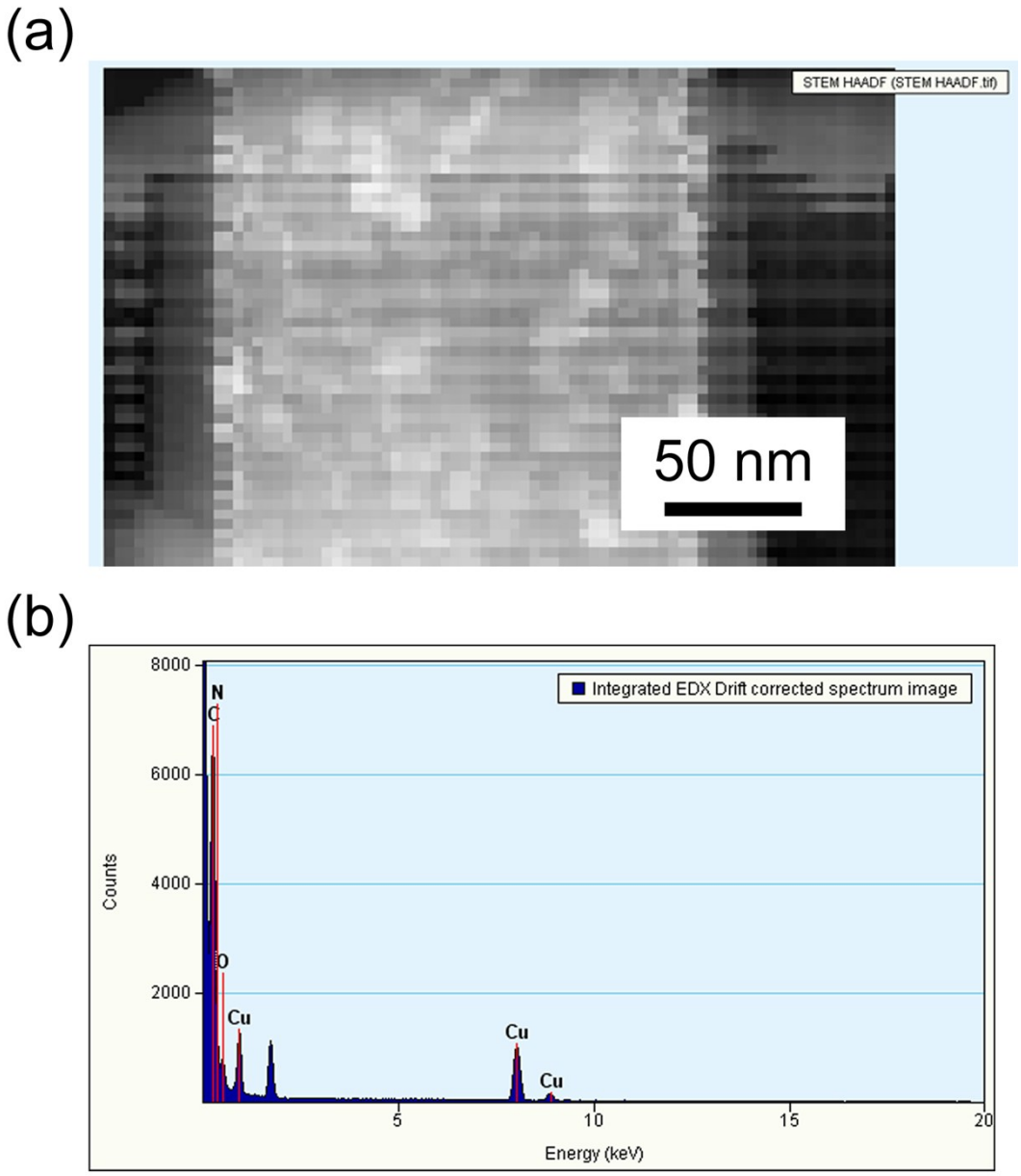

Fig. S4 The selected area of TEM images about EDX mapping (a) and corresponding energy dispersive X-ray spectra (EDS) analysis (b) related to Fig. 2f.

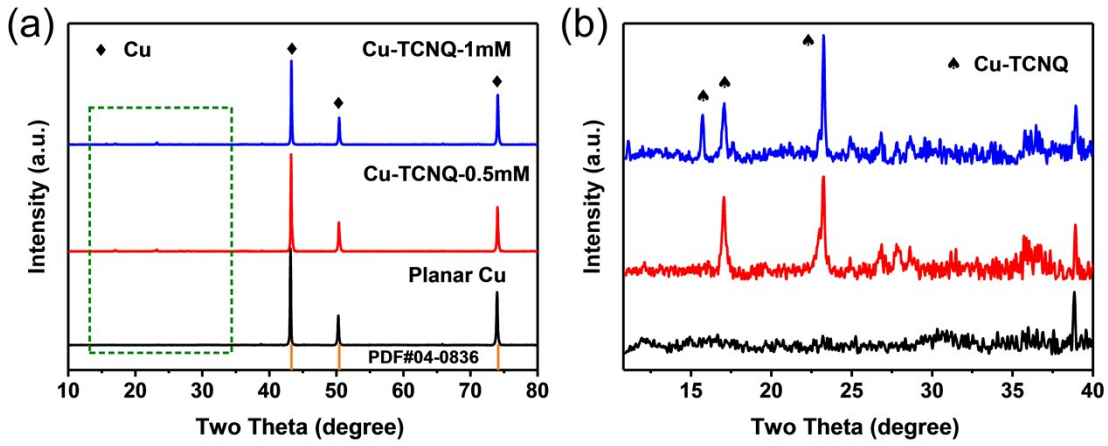

Fig. S5 (a) XRD pattern of planar Cu foil and Cu-TCNQ/CF with different concentration of TCNQ acetonitrile solution. (b) Enlarge pattern of the green dotted box.

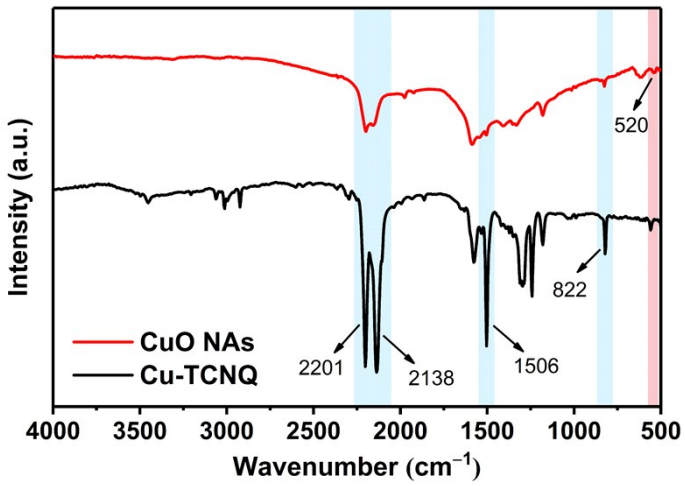

Fig. S6 FT-IR spectra of Cu-TCNQ and CuO NAs.

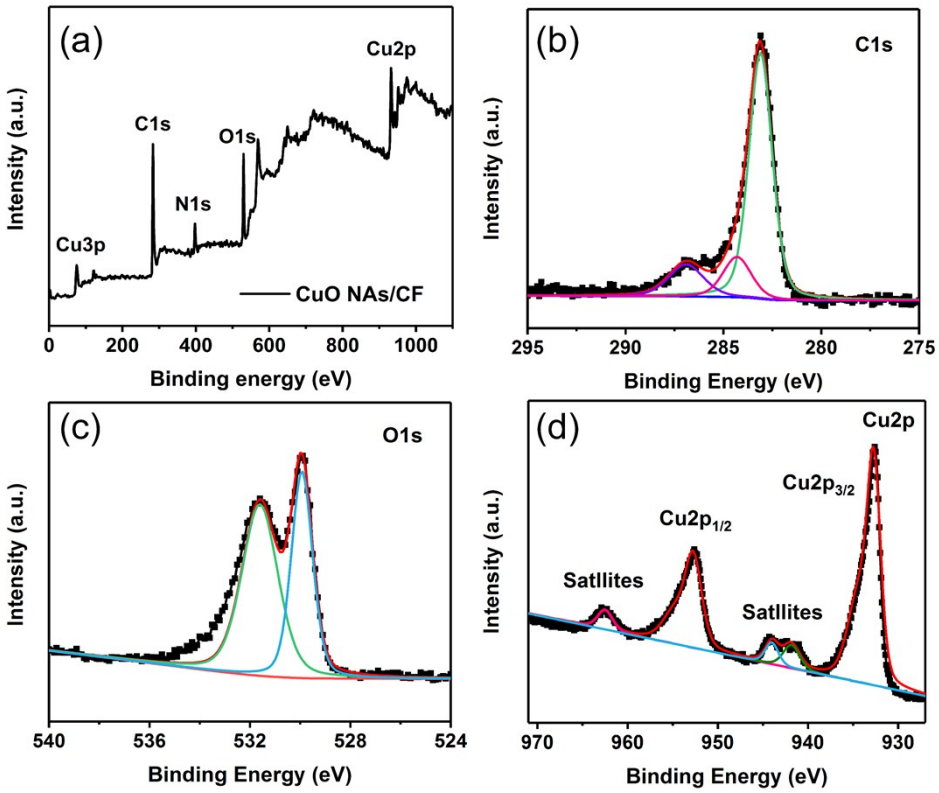

Fig. S7 XPS and corresponding high resolution spectra of (a) CuO NAs/CF, (b) C1s (c) O1s, (d) Cu2p.

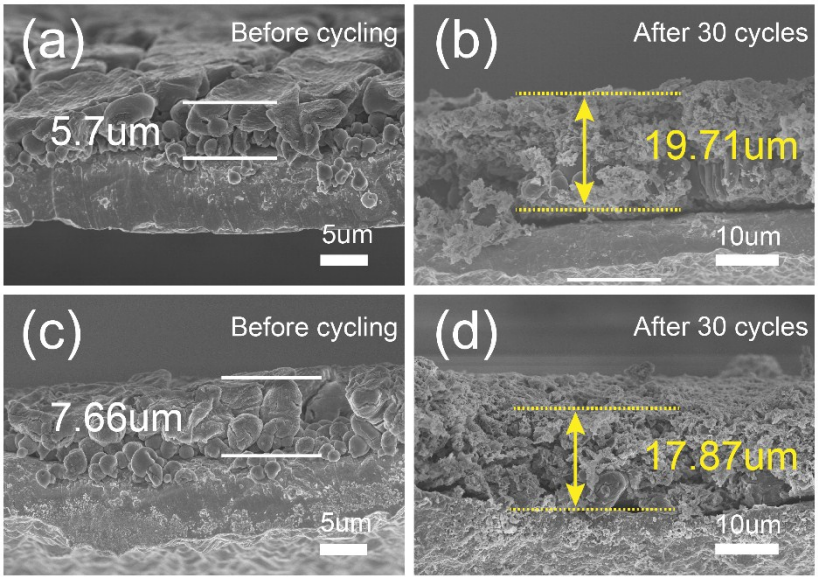

Fig. S8 Cross-section SEM images of Li deposited on bare foil (a, b) and CuO NAs/CF (c, d). Before cycling (a, c), after 30th cycles (b, d).

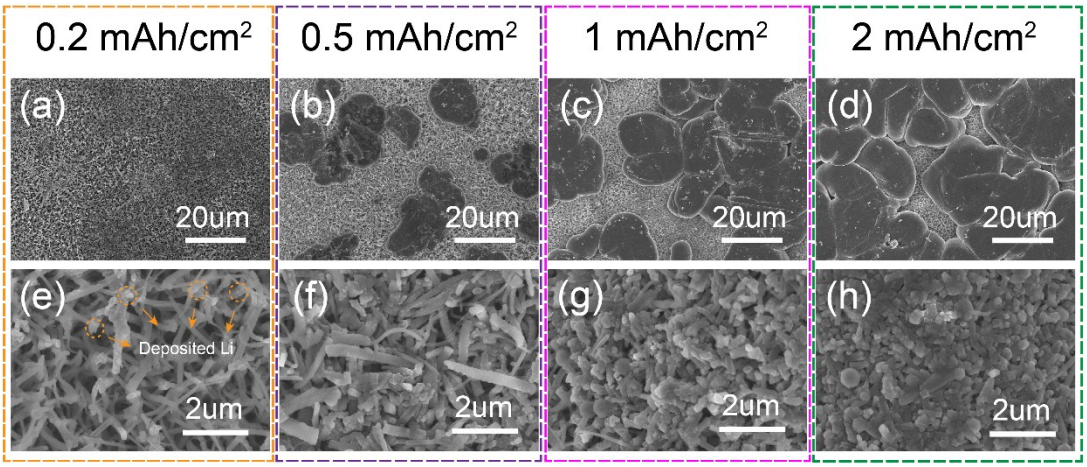

Fig. S9 Top view SEM images of Li deposited morphologies on CuO NAs/CF current collector with different amounts of Li deposition capacities at 1mA cm^{-2}.(a, e) 0.2 mA h cm^{-2}, (b, f) 0.5 mA h cm^{-2}, (c, g) 1 mA h cm^{-2}, (d, h) 2 mA h cm^{-2}. The deposited Li were labeled by orange arrows.

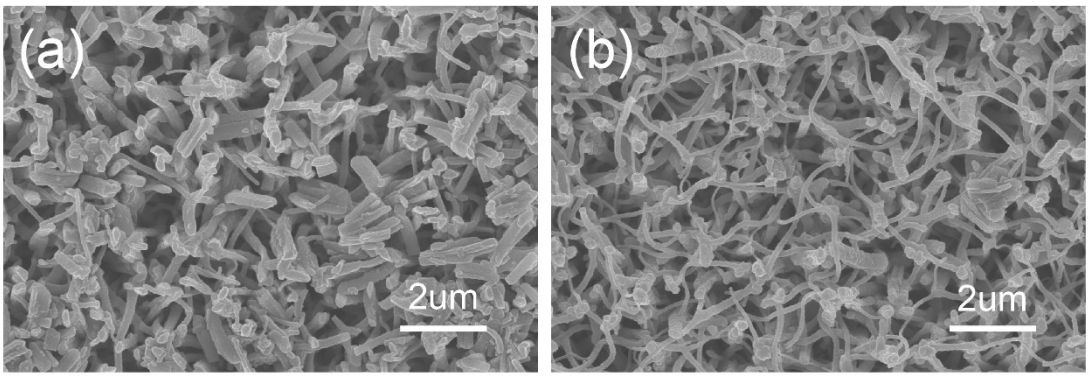

Fig. S10 Top view SEM images of Li deposited on CuO NAs/CF current collector after 10 cycles.

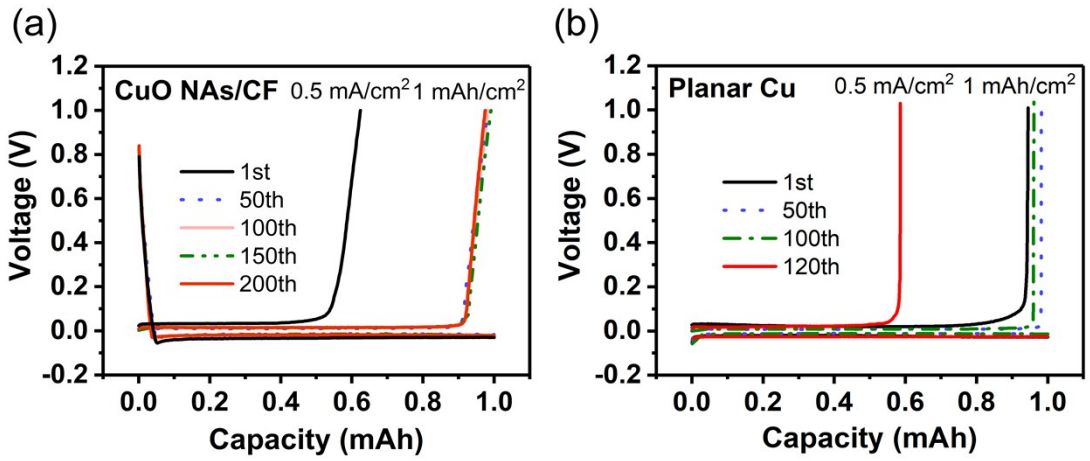

Fig. S11 Voltage-capacity curves of Li plating/stripping process on (a) CuO NAs/CF and (b) planar Cu foil current collector at 0.5 mA cm^{-2} for 1 mA h cm^{-2} of Li.

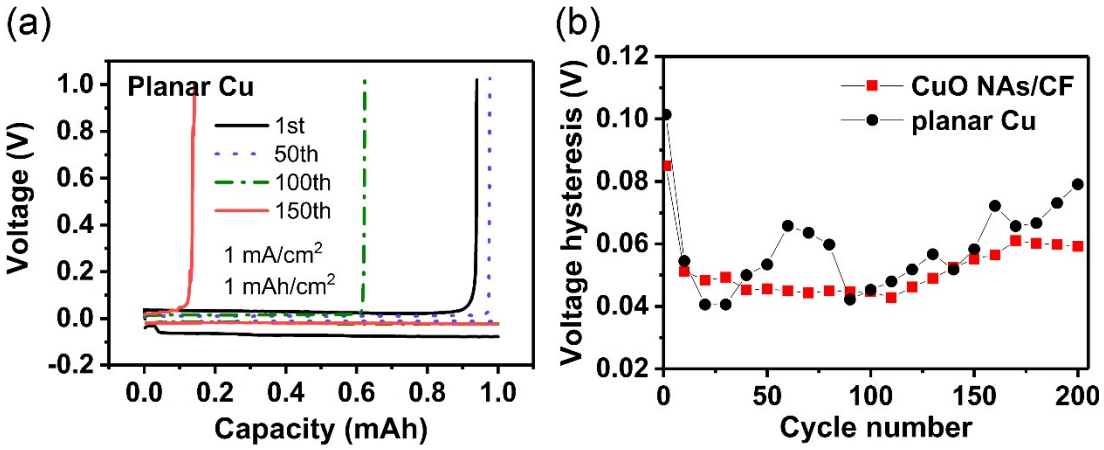

Fig. S12 (a) The voltage-capacity curves of Li plating/stripping process at various cycles under 1 mA/cm^2 for a total capacity of 1 mA h cm^{-2} Li. (b) Comparison of voltage hysteresis for 200 cycles at a current density of 1 mA cm^{-2}.

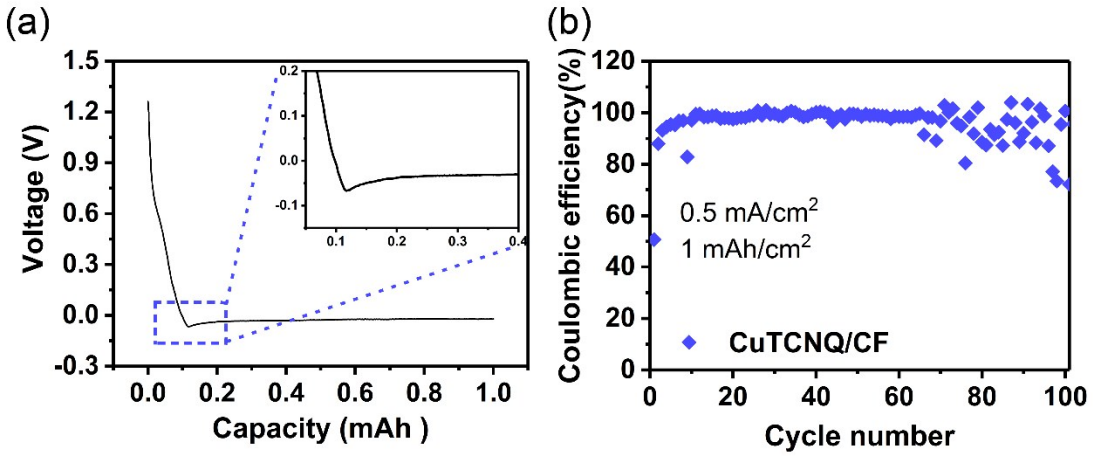

Fig. S13 (a) Voltage profiles of Li nucleation on Cu-TCNQ/CF current collector at a current density of 0.5 mA cm^{-2}. (b) Coulombic efficiency of Cu-TCNQ/CF current collector at 0.5 mA cm^{-2} with a total capacity of 1 mA h cm^{-2}.

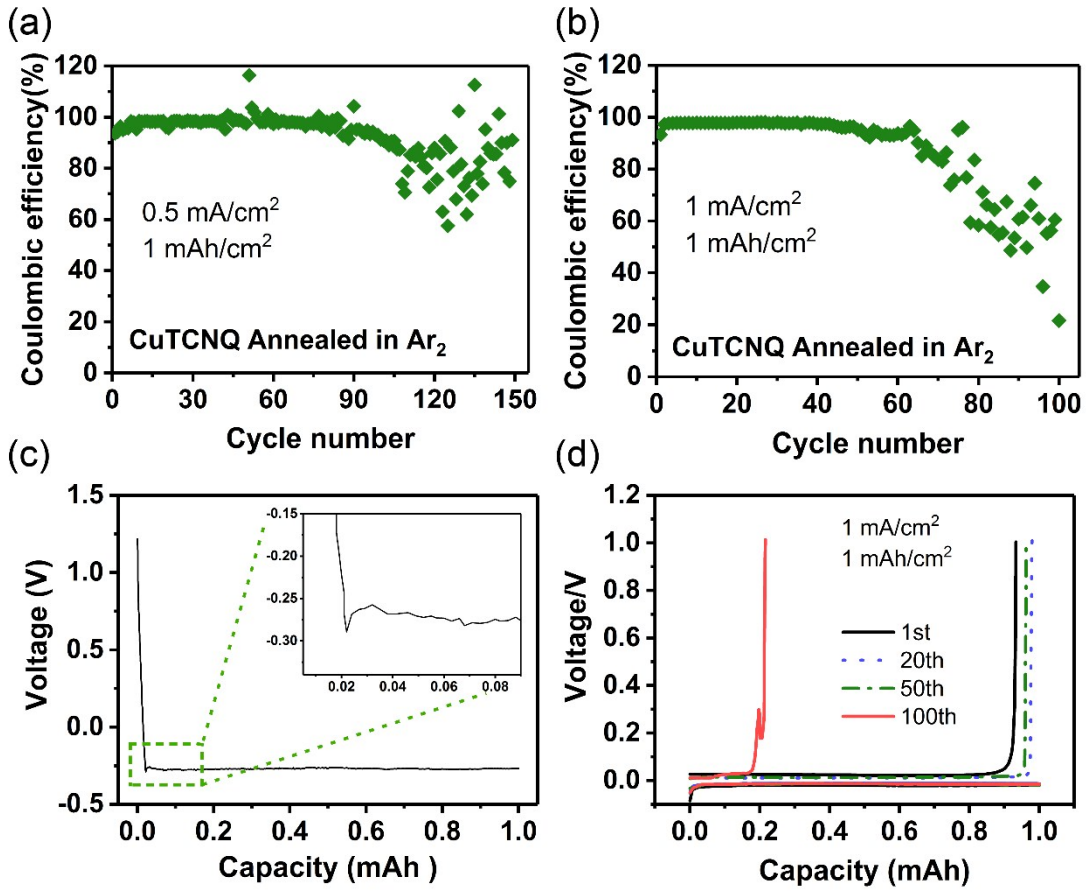

Fig. S14 Coulombic efficiency of cells using the current collector that Cu-TCNQ/CF annealed in Ar_2 with 1 mA h cm^{-2} at a current density of (a) 0.5 mA cm^{-2}, (b) 1 mA cm^{-2}. (c) Voltage profiles of Li nucleation on the current collector at 0.5 mA cm^{-2}. (d) The corresponding voltage-capacity

curves of Li plating/stripping process at 1 mA cm^{-2} for 1 mA h cm^{-2} of Li.

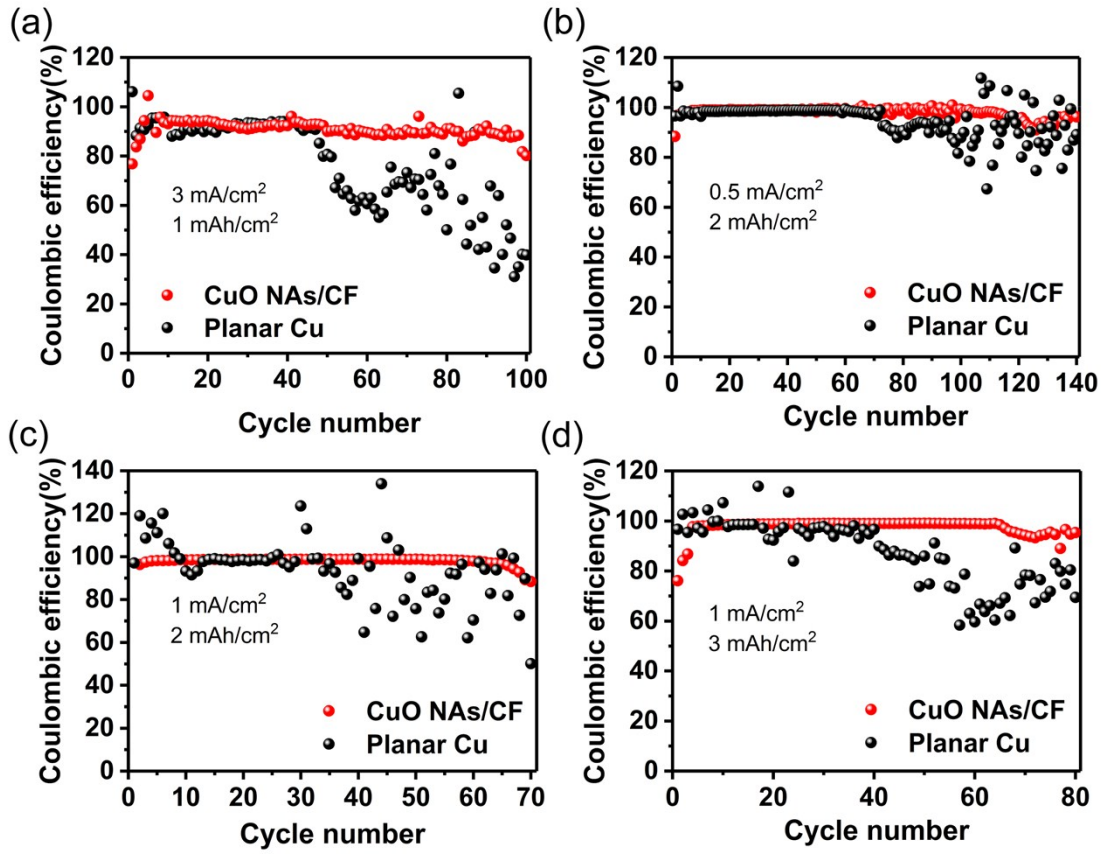

Fig. S15 (a) Coulombic efficiency of CuO NAs/CF and planar Cu foil current collector with 1 mA h cm^{-2} capacity at a current density of 3 mA cm^{-2}. Coulombic efficiencies of two current collectors with a capacity of 2 mA h cm^{-2} at (b) 0.5 mA cm^{-2}, (c) 1 mA cm^{-2}. (d) Coulombic efficiency of two current collectors with a capacity of 3 mA h cm^{-2} at 1 mA cm^{-2}.

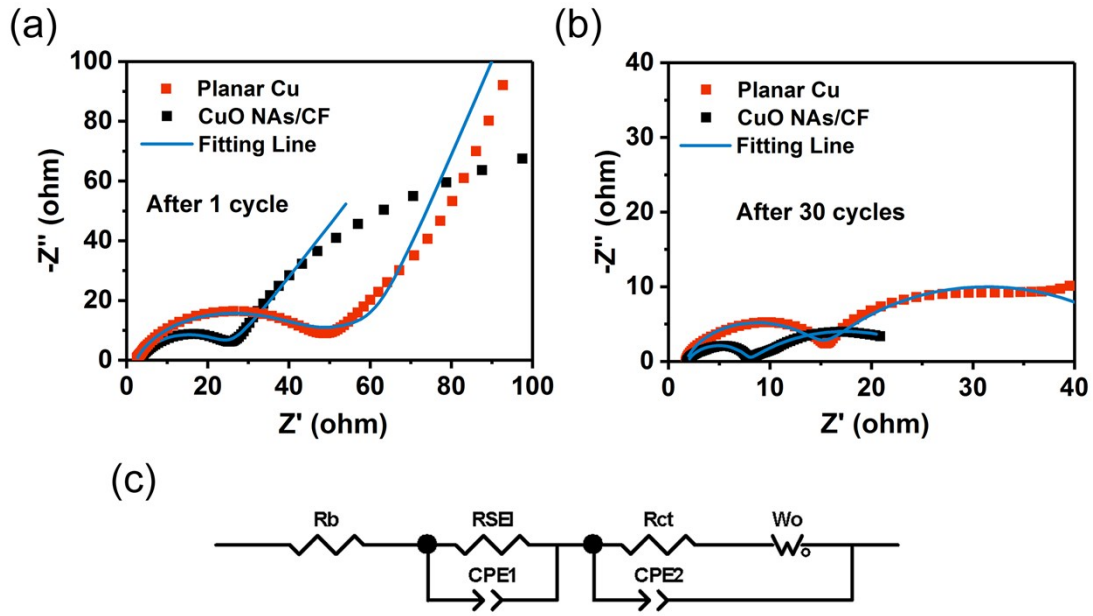

Fig. S16 Electrochemical impedance spectra (EIS) of Planar Cu foil and CuO NAs/CF after (a) 1st cycle (b) 30th cycles. (c) Equivalent circuit diagram for EIS plots in (a) and (b).

In addition, the electrochemical impedance was also fitted with Z-View software and the fitted parameters were shown in Table S1. It is shown that the bulk resistance (R_b) increases after cycling. The charge transfer resistance (R_{ct}) for the CuO NAs/CF is about 24.21 Ω after the 1st cycle and then decreases to 19.24 Ω after the 30th cycles, much lower than that of the planar Cu.

Table S1. Electrochemical impedance fitted parameters for **Figure S16 (**a**)** and (b) with an equivalent circuit model.

	Planar Cu			CuO NAs/CF		
	R_b (Ω)	R_{SEI} (Ω)	R_{ct} (Ω)	R_b (Ω)	R_{SEI} (Ω)	R_{ct} (Ω)
1 cycle	1.561	-	44.19	1.748	-	24.21
30 cycles	1.709	13.18	33.2	1.913	5.899	19.24

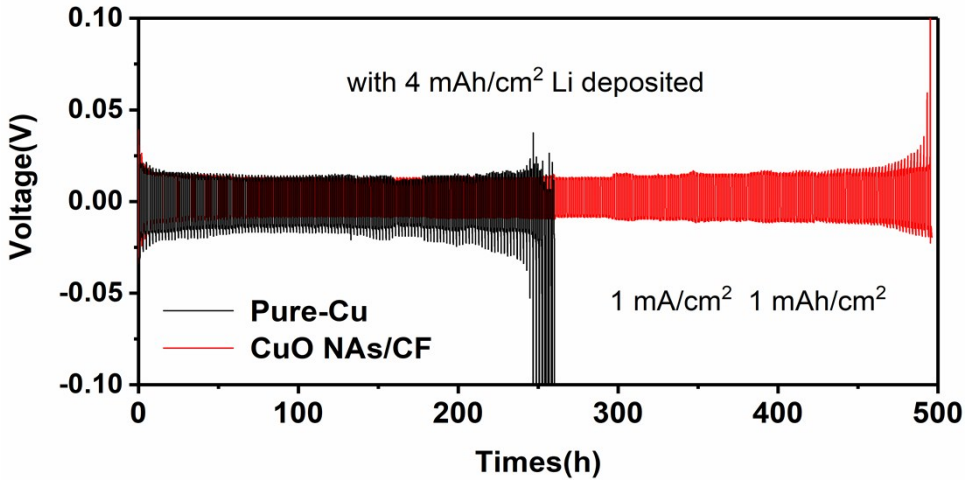

Fig. S17 Voltage-time profiles of the symmetric cells for Li plating or stripping at 1 mA cm^{-2} for 1 mA h cm^{-2} with 4 mA h cm^{-2} pre-deposited Li.

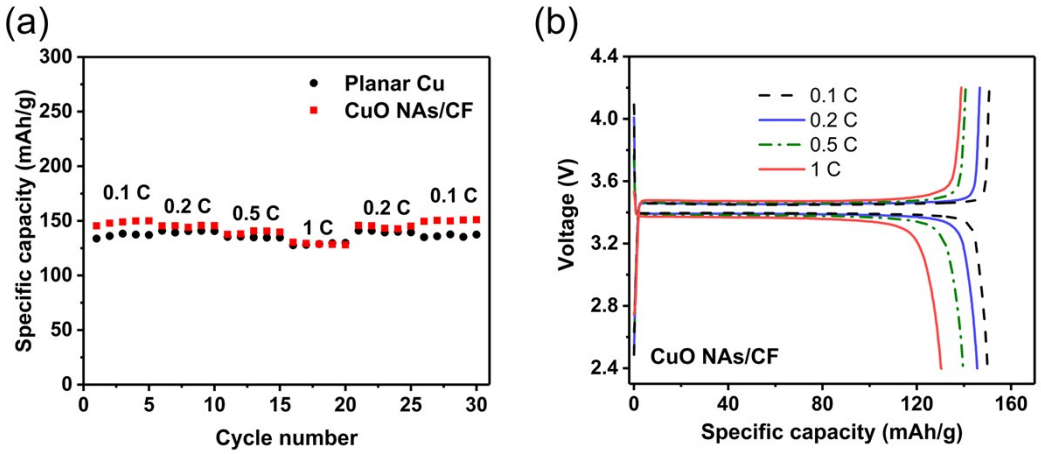

Fig. S18 (a) The rate performance of $LiFePO_4$ full cells using planar Cu foil and CuO NAs/CF. (b) Charge-discharge curves of the Li-CuO NAs/CF||LFP full cells cycled at various C rates between 0.1 and 1C.

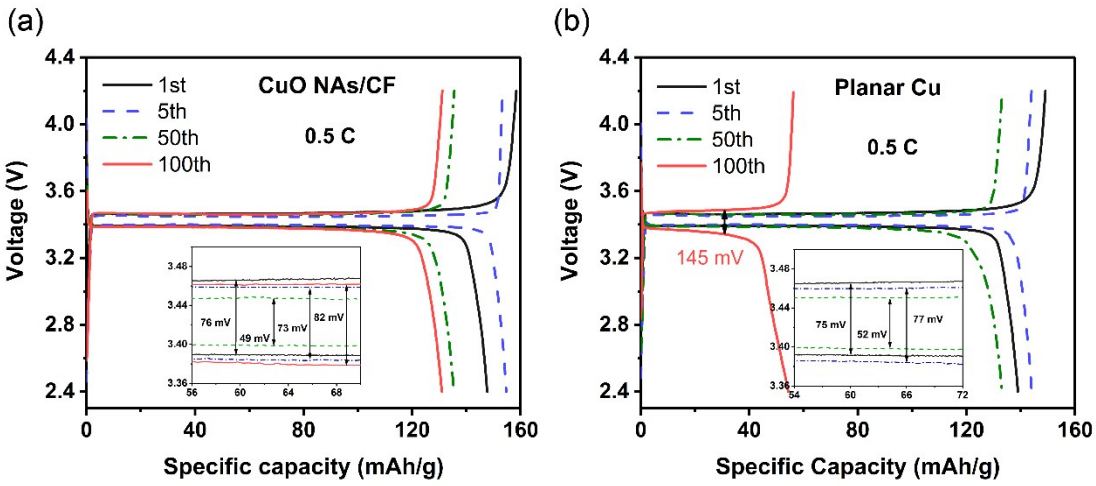

Fig. S19 Typical galvanostatic charge-discharge profiles of the CuO NAs/CF||LFP and Li-Cu||LFP full cells at 0.5C.